Effect of an open crack on the output parameters of a heterojunction solar cell

Amina ENNEMRI
Energetic and Mechanical Engineering Laboratory
UMBB
Boumerdès, Algeria
ennemriamina@gmail.com

Halima MAZOUZ
Saad Dahlab University
Renewable Energies Department
Blida, Algeria
halima.mazouz@yahoo.fr

Ali KHOUZAM
Univ Paris-Est Créteil, CERTES
ICAM Grand-Paris Sud
Lieusaint, France
ali.khouzam@icam.fr

Pierre-Olivier LOGERAIS
Univ Paris-Est Créteil, CERTES
Lieusaint, France
pierre-olivier.logerais@u-pec.fr

***Abstract*— Photovoltaic modules suffer from degradations under operating conditions, and equally during transportation, installation and maintenance. Among common degradation modes, cracks represent an important alteration factor for photovoltaic panels. Actually, their connection to the efficiency loss of a photovoltaic module has not been well established yet. In the present study, the impact of the depth of an open crack within a heterojunction solar cell was studied using a finite element model. Steady-state simulations of the PN junction were carried out for a depth ranging from 0 to 5 µm. A linear decrease is obtained for the short-circuit current and, an important drop of the open-circuit voltage is found between 0 and 0.25 µm depth. The efficiency is significantly reduced, from 19.97% to 12.94%, with a crack depth of 5 µm.**

Keywords — PN junction, heterojunction solar cell (HJ), open crack, modeling, output parameters

I. INTRODUCTION

The most sensitive component of a photovoltaic (PV) system is the solar cell, which can be prone to cracking as a result of various manufacturing processes and operating conditions [1,2]. Indeed, the presence of cracks can lead to a decrease in the energy produced over time by a photovoltaic module and can also induce other degradations such as corrosion, delamination, hot spots, snail trails or discoloration [3-6]. They are discernible mainly at the surface of a photovoltaic cell, at the beginning and at the end of the busbars or along them [7,8]. The interconnecting ribbon between the solar cells, another critical part of a solar PV module assembly, can also be affected by the presence of cracks. This ribbon failure negatively impacts the performance and reliability of the entire PV module [9].

Experimental or modeling approaches have been used to study the microcracks in solar cells in view of determining their number, orientation, position and frequency, as well as to relate these parameters to the engendered power loss [10], [11]. When cracks appear in a solar cell, the parts separated from the cell might not be totally disconnected. However, the series resistance across the crack varies as a function of the distance between the cell parts and the number of cycles for which the PV module is deformed [12]. Nevertheless, when a cell part is fully isolated, the current decrease is proportional to the disconnected area [13].

In the study of Kajari-Schröder et al., a power reduction of around 25% was attributed to the presence of a single crack having a parallel orientation in a silicon solar cell [7]. The appearance of cracks under the effect of thermal cycles was observed at the interconnection of the soldering joints in the study of Subrahmanyan et al., who obtained an increase in the series resistance which led to a reduction in the fill factor and the power generated by the solar cells [14]. Moreover, a simulation study based on field data handled by Morlier et al. estimated the power loss of multicrystalline silicon modules between 6 and 22% in the presence of cracks [12]. In another work, a multi-physics and multi-scale numerical approach showed that the evolution of microcracks in polycrystalline silicon solar cells had an impact on their electrical responses resulting in significant power losses [13]. It was reported, in particular, that the fill factor decreased from 65% to 15% for a micro-cracked module.

The case of a heterojunction solar cell (HJ) a-Si /c-Si is chosen for the present study as this technology offering intrinsic advantages and better temperature coefficients compared to a traditional homojunction c-Si cell is promising [15,16]. In fact, it combines both the performance of a crystalline silicon cell and the low heat balance of a thin amorphous silicon layer, owing to which HJ solar cells have been the focus of intensive research in the field of photovoltaic solar cells [17]. Unlike crystalline silicon homo-junction photovoltaic cells where photovoltaic cell cracking has been moderately addressed, the impact on the performance of hetero-junction photovoltaic cells is not well known.

The purpose of this study is to investigate the effects of an open crack on the performance of a heterojunction (HJ) solar cell composed of a-Si (p) / c-Si (n) under the AM 1.5 spectrum. Specifically, the study aims to model the presence of an open crack with varying thicknesses and analyze its impact on the output parameters of the solar cell. The study utilized a 2D finite element model to simulate the degraded characteristics and to examine the relationship between the crack depth and the decline in the electrical output parameters.

II. MODEL OF THE HETEROJUNCTION SOLAR CELL

The structure, the mesh, the equations, the data of the model and the boundary conditions for the simulation are depicted in this section. An open crack is considered within a two-dimensional representation of a PN junction.

A. Structure

Figure 1 shows the structure of the a-Si/c-Si solar cell studied which consists of a thin film of highly doped amorphous silicon a-Si (p) and a moderately doped monocrystalline silicon wafer c-Si (n). The thickness of the absorber layer c-Si (n) is 300 µm and the one of the emitter layer a-Si (p) is 2 µm. A finite element model of the PN junction was constructed for a healthy junction and for a junction with an open crack of 1 µm width having a depth ranging from 0 to 5 µm. This approach made it possible to assess the situation for which the crack is inside the emitter and the one for which it is located both inside the emitter and in the base. This way, the modified depletion region area is taken into account.

B. Mesh

The generated mesh of the PN junction is shown in Figure 2 for the case of a healthy cell and for a deteriorated one. The wide range of carrier concentrations makes the numerical simulation of the semiconductor equations a difficult task. For this reason, we carefully generated a denser mesh around the depletion region, at the anode and at the cathode. The maximum element size is of 1×10^{-7} m^2 and the mesh has 3684 elements.

C. Equations

The charge carrier continuity and the space-charge effect are solved by a coupled resolution based on Poisson's equation (1), the equation of continuity for electrons (2) and for holes (3) [17]. The following equations are applied for the x direction:

$$-\nabla.(\varepsilon.\nabla\psi) = q.(p - n + N) \quad (1)$$

$$\frac{dJ_n}{dx} = -q.\left(G_{opt} - R\right) \quad (2)$$

$$\frac{dJ_p}{dx} = q.\left(G_{opt} - R\right) \quad (3)$$

where for equation (1), Ψ is the electrostatic potential, n and p are the electron and the hole concentrations respectively; ε is the dielectric permittivity; q is the elementary charge; N represents the fixed charge associated with the ionized donors. On the other hand, in equations (2) and (3), J_n and J_p are the electron and hole conduction current densities; G_{opt} is the optical generation; R is the sum of band-to-band recombination and Auger recombination.

The generation of the free carriers is an optical generation G_{opt}:

$$G_{opt} = (1 - r).\alpha(\lambda).\phi(\lambda)\exp\ (-\alpha(\lambda).x) \quad (4)$$

where r is the reflectivity of the front contact, $\phi(\lambda)$ is the flux of incident photons of wavelength λ, and $\alpha(\lambda)$ is the spectral absorption coefficient [17].

D. Physical data

The material properties used in the model are detailed in Table 1.

E. Boundary conditions

Equations (1)-(3) were solved assuming the continuity of the electric potential and electric field at the interface (ii). For boundaries far from the component active zones, the normal electric field component and the carrier densities were all taken equal to zero. For electrical contacts, the electric potential was considered at 0.5 V for boundary (i) touching metal and at 0 V at the back for boundary (iii). Infinite recombination velocity on these surfaces was assumed. A symmetrical condition with null charge was specified for the side walls (boundary (iv)) as only a portion of the PV cell was modeled.

TABLE I. MATERIAL PROPERTIES [14]

Parameters	a-Si(p)	c-Si(n)
Thickness (µm)	2	300
Band gap (eV)	1.72	1.124
Auger recombination coefficient for electrons ($cm^6.s^{-1}$)	0	2.2×10^{-31}
Auger recombination coefficient for holes ($cm^6.s^{-1}$)	0	9.9×10^{-32}
Direct band-to-band recombination coefficient ($cm^6.s^{-1}$)	0	1.1×10^{-14}
Electron mobility ($cm^2.V^{-1}.s^{-1}$)	25	1040
Hole mobility ($cm^2.V^{-1}.s^{-1}$)	5	412
Dielectric constant	11.9	11.9

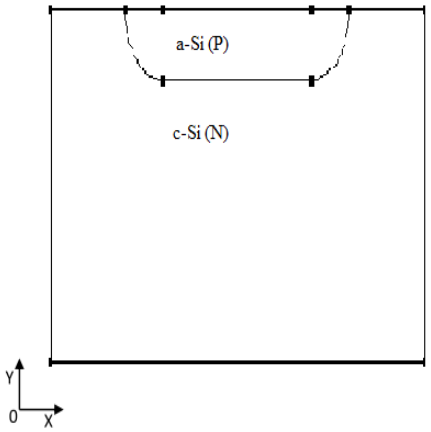

Fig. 1. Structure of the simulated heterojunction solar cell.

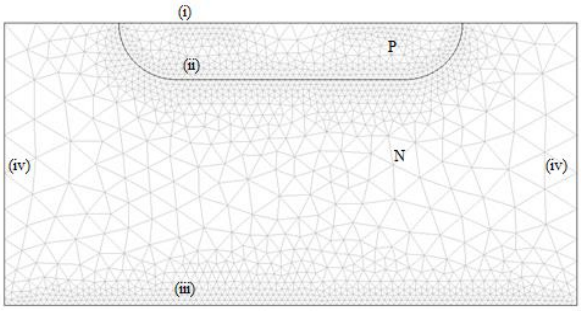

a) Healthy cell

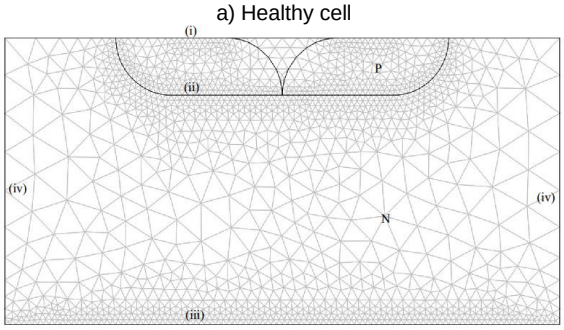

b) Cell with an open crack of 2 µm depth

Fig. 2. Mesh of the intact and cracked heterojunction cell.

These conditions were defined for the reference case, noted (a), of a junction without cracking. The other two situations were:

- Case (b): depth of crack between 0 and 2 µm, in other words, cracking only in the emitter a-Si layer;
- Case (c): depth of crack superior to 2 µm, in other words, cracking in both layers a-Si (p) and c-Si (n).

For cases (b) and (c), the electric potential is considered at 0.5 V for the crack limit and the choice of the depth of the crack was chosen arbitrarily up to 5 µm.

III. CALCULATIONS

A. Numerical simulations

The silicon solar cell was simulated under Standard Test Conditions: an exposure under an atmosphere of Air Mass 1.5 (AM1.5) for which the integral power density is 1000 W/m^2 and the cell temperature 25° C.

The solar spectrum was introduced into the simulator by an input database. Calculations were performed for the steady-state case. Lagrange quadratic elements (integration order of 4 and constraint order of 2) were used. Calculations were carried out with the finite-element resolution COMSOL Multiphysics software, taking into account the electrostatic and the diffusion modules [18].

B. Calculation of the output parameters

The open-circuit voltage (V_{oc}) is the maximum voltage that the solar cell supplies in the absence of a load, and the short-circuit current (I_{sc}) is the maximum current of the solar cell with a zero resistance load. The Fill Factor (FF) is the ratio between the maximum power P_{max} and the product of I_{sc} by V_{oc}:

$$FF = \frac{P_{max}}{I_{sc}.V_{oc}} \quad (5)$$

Considering the short-circuit current and the maximum densities, noted J_{sc} and J_m, equation (5) can be written as:

$$FF = \frac{J_m.V_m}{J_{sc}.V_{oc}} \quad (6)$$

The power conversion efficiency (PCE) η is the primary parameter extracted from the I-V curve which describes the general efficiency of the solar cell that is the ratio of the generated electricity to the incoming light energy. The formula to find out the PCE is [19]:

$$\eta = \frac{J_{sc}.V_{oc}.FF}{P_{light}} \quad (7)$$

where P_{light} is the incident light power (in W/m^2).

IV. RESULTS AND DISCUSSION

A. Analysis of the electrical characteristics of the healthy solar cell

A numerical simulation was first carried out in the absence of a crack as a reference case. The $J(V)$ characteristic of the basic a-Si(p)/c-Si(n) heterojunction cell simulated under the standard AM1.5 spectrum is given in Figure 3. The output parameters were extracted from this $J(V)$ characteristic: the density of short-circuit current J_{sc} was 32.27 mA/cm^2, the open-circuit voltage V_{oc} 0.7867 V, the fill factor FF 77.93% and the efficiency η 19.79%.

B. Analysis of the electrical characteristics of the cracked solar cell

The characteristics and the output parameters of the heterojunction cell with the presence of the crack with the distinctive depths were calculated. The case of an uncracked cell is indicated for comparison.

The evolution of the current density versus voltage for the different depths of the open crack is provided in Figure 4, as well as the power. A clear deterioration in the output parameters can be noticed. By increasing the depth of the crack, the electrical characteristic of the solar cell is degraded. J_{sc} decreases significantly according to the depth, whereas V_{oc} remains approximately constant but is reduced compared to the healthy solar cell. The appearance of a crack causes a loss in the open-circuit voltage.

The reductions of the short-circuit current density J_{sc}, the open-circuit voltage V_{oc} and the power conversion efficiency η were plotted with respect to the depth of the crack in the graphs of Figure 5. The relative reduction in the efficiency was calculated in Table 2 using the expression below:

$$Reduction\ of\ \eta\% = \frac{\eta_0 - \eta_c}{\eta_0} \times 100 \quad (8)$$

where η_0 is the efficiency of the cell without a crack and η_c is the efficiency of the cracked cell.

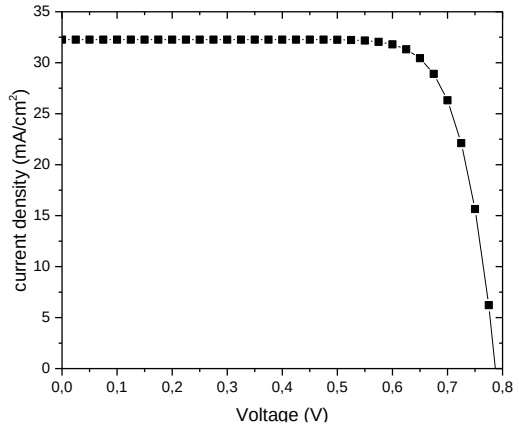

Fig. 3. J(V) characteristics of healthy a-Si(p)/c-Si(n) junction.

TABLE II. OUTPUT PARAMETERS OF THE SOLAR CELL WITH DIFFERENT CRACK DEPTHS.

Crack depth (µm)	0	0.25	0.5	1.0	1.5	2.0	2.5	5.0
J_{sc} (mA/cm²)	32.27	30.95	30.64	30.21	29.84	29.57	28.31	26.67
V_{co} (V)	0.787	0.691	0.690	0.689	0.688	0.687	0.681	0.677
FF	77.93	71.02	71.06	71.13	71.15	71.19	71.49	71.64
η%	19.79	15.19	15.03	14.80	14.60	14.46	13.79	12.94
Reduction of η%	0	23.23	24.06	25.20	26.22	26.94	30.29	34.62

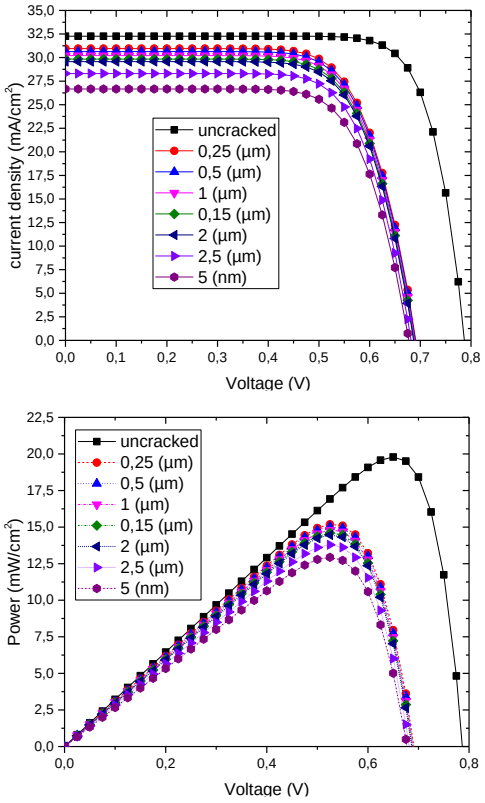

Fig. 4. Evolution of the (a) current density–voltage *J(V)* and (b) power–voltage P(V) characteristics according to the crack depths.

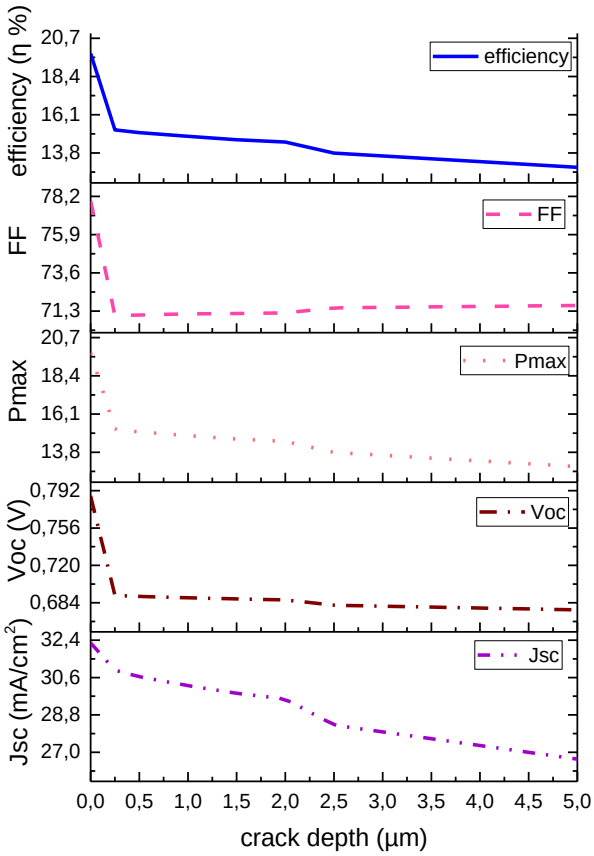

Fig. 5. Effects of the crack depth on the performance of the heterojunction solar cell.

The efficiency decreased from 19.79% to 15.19% for the smallest crack depth (0.5 µm) and 12.94 % for the deepest (5 µm) corresponding to a 23.23% and 34.62% reduction. This could be explained by the fact that in the case of cracking, there exist inactive or less active zones with fewer carriers available and also a low incident power of the light to produce current in the cell.

The simulated output results depicted in Figure 5 show some remarkable behaviors: a strong variation of the output parameters for crack depths between 0 and 0.25 µm followed by linear degradations for crack depths between 0.25 and 2 µm, the slopes being of -0.0417, -0.00023 and -0.0788 for η, V_{oc} and J_{sc} respectively. The decrease between 2 and 2.5 µm is also regular but more important due to the influence of the depletion region. Beyond 2.5 µm depth, the slopes are of -0.034, -0.00016 and -0.0656 for η, V_{oc} and J_{sc}. respectively.

These degradations of the output parameters can be justified with an experimental analysis of the cracks in the silicon-based cell (mono and polycrystalline) [20,21]. Furthermore, cracks in the HJ cells can cause poor contact

between the busbar and the fingers, increasing the contact resistance. In addition, they can engender a raise in the series resistance [22] and reduce to a small extent the V_{oc} [23,24].

The findings of this study will be beneficial for the management of photovoltaic installations and smart grids in several ways. Foremost, they will enable the development of efficient maintenance strategies to mitigate the impact of cracks, ensure optimal performance and maximize the energy yield of solar installations. Secondly, the results will contribute to the design and improvement of solar cell manufacturing processes, leading to enhanced quality control measures and durability of solar cells.

Moreover, this study explored the relationship between the depth of a crack and the decrease in electrical output parameters, thus providing valuable knowledge to the system designers and the network operators. This understanding can guide the implementation of preventive measures, such as early fault detection systems, to promptly identify and address issues related to crack-induced performance degradation.

V. Conclusion

A heterojunction solar cell of a-Si (p) / c-Si (n) under the AM 1.5 spectrum was modeled with the presence of an open crack having different thicknesses. A 2D finite element model was realized to simulate the degraded characteristics.

The results of the simulation show that a crack causes the lowering of the output parameters of the HJ solar cell. The PV cell had initially an efficiency of 19.79%, an open-circuit voltage V_{oc} of 0.7867 V and a density current J_{sc} of 32.27 mA/cm^2. For the cracked cell of 5 µm depth, the efficiency was reduced to 12.94%, the open-circuit voltage to 0.6772 V and the current density to 26.76 mA/cm^2. A proportional relationship between the declination of the electrical output parameters and the crack depth was found beyond a depth of 0.25 µm.

Acknowledgment

The authors extend their sincere thanks to Mrs. Wilhelmina Logerais, a native English speaker, for proofreading this article.

References

[1] G. Goudelis, P. I. Lazaridis, and M. Dhimish, “A Review of Models for Photovoltaic Crack and Hotspot Prediction,” *Energies*, vol. 15, no. 12, 2022.

[2] A. Ennemri, P.-O. LOGERAIS, M. Balistrou, J. F. Durastanti, and I. BELAIDI, “Cracks in silicon photovoltaic modules: a review,” *J. Optoelectron. Adv. Mater.*, vol. 21, no. 1–2, pp. 74–92, 2019.

[3] A. Ndiaye, A. Charki, A. Kobi, C. M. F. Kébé, P. A. Ndiaye, and V. Sambou, “Degradations of silicon photovoltaic modules: A literature review,” *Sol. Energy*, vol. 96, pp. 140–151, 2013.

[4] D. C. Jordan, C. Deline, S. R. Kurtz, G. M. Kimball, and M. Anderson, “Robust PV Degradation Methodology and Application,” *IEEE J. Photovoltaics*, vol. 8, no. 2, pp. 525–531, 2018.

[5] V. Sharma and S. S. Chandel, “Performance and degradation analysis for long term reliability of solar photovoltaic systems: A review,” *Renew. Sustain. Energy Rev.*, vol. 27, pp. 753–767, 2013.

[6] A. Dolara, G. C. Lazaroiu, S. Leva, G. Manzolin, and L. Votta, “Snail Trails and Cell Micro-Cracks impact on PV module maximum power and energy production,” *IEEE J. Photovoltaics*, vol. 6, no. 5, pp. 1269–1277, 2016.

[7] S. Kajari-Schröder, I. Kunze, U. Eitner, and M. Köntges, “Spatial and orientational distribution of cracks in crystalline photovoltaic modules generated by mechanical load tests,” *Sol. Energy Mater. Sol. Cells*, vol. 95, no. 11, pp. 3054–3059, 2011.

[8] N. Park, J. Jeong, and C. Han, “Estimation of the degradation rate of multi-crystalline silicon photovoltaic module under thermal cycling stress,” *Microelectron. Reliab.*, vol. 54, no. 8, pp. 1562–1566, 2014.

[9] A. Eslami Majd and N. N. Ekere, “Crack initiation and growth in PV module interconnection,” *Sol. Energy*, vol. 206, pp. 499–507, 2020.

[10] M. Köntges, I. Kunze, S. Kajari-Schröder, X. Breitenmoser, and B. Bjørneklett, “The risk of power loss in crystalline silicon based photovoltaic modules due to micro-cracks,” *Sol. Energy Mater. Sol. Cells*, vol. 95, no. 4, pp. 1131–1137, 2011.

[11] S. Kajari-Schröder, I. Kunze, and M. Köntges, “Criticality of cracks in PV modules,” *Energy Procedia*, vol. 27, pp. 658–663, 2012.

[12] A. Morlier, F. Haase, and K. Marc, “Impact of Cracks in Multicrystalline Silicon Solar Cells on PV Module Power — A Simulation Study Based on Field Data,” pp. 1–7, 2015.

[13] M. Paggi, M. Corrado, and M. A. Rodriguez, “A multi-physics and multi-scale numerical approach to microcracking and power-loss in photovoltaic modules,” *Compos. Struct.*, vol. 95, pp. 630–638, 2013.

[14] R. Subrahmanyan, J. R. Wilcox, and C.-Y. Li, “A damage integral approach to thermal fatigue of solder joints,” *IEEE Trans. Components, Hybrids, Manuf. Technol.*, vol. 12, no. 4, pp. 480–491, 1989.

[15] W. Fuhs, K. Niemann, and J. Stuke, “Heterojunctions of Amorphous Silicon and Silicon Single Crystals,” *AIP Conf. Proceedings,New York*, vol. 345, no. 1, 1974.

[16] Mikio Taguchi, Akira Terakawa, Eiji Maruyama, Makoto Tanaka, “Obtaining a Higher Voc in HIT Cells,” *Prog. Photovoltaics Res. Appl.*, no. 13, pp. 481–488, 2005.

[17] H. Mazouz, P. O. Logerais, A. Belghachi, O. Riou, F. Delaleux, and J. F. Durastanti, “Effect of electron irradiation fluence on the output parameters of GaAs solar cell,” *Int. J. Hydrogen Energy*, vol. 40, no. 39, pp. 13857–13865, 2015.

[18] COMSOL Multiphysics, “Documentation for COMSOL release 3.4.,” *MA, USA COMSOL*, p. aviable: http://www.comsol.com., 2008.

[19] E. Lorenzo, “Solar electricity: engineering of photovoltaic systems,” 1994, pp. 59–85.

[20] I. Maria and E. Molina, “Crack Analysis in Silicon Solar Cells,” 2012.

[21] M. Dhimish, V. D'Alessandro, and S. Daliento, "Investigating the Impact of Cracks on Solar Cells Performance: Analysis Based on Nonuniform and Uniform Crack Distributions," *IEEE Trans. Ind. Informatics*, vol. 18, no. 3, pp. 1684–1693, 2022.

[22] Sylvain De Vecchi, "hétérojonction de silicium et contacts interdigités en face arrière To cite this version : Développement de cellules photovoltaïques à hétérojonction de silicium et contacts interdigités en face arrière," INSA de Lyon, 2013.

[23] A. Augusto, K. Tyler, S. Y. Herasimenka, and S. G. Bowden, "Flexible Modules Using <70 μm Thick Silicon Solar Cells," *Energy Procedia*, vol. 92, pp. 493–499, 2016.

[24] A. Augusto, P. Balaji, H. Jain, S. Y. Herasimenka, and S. G. Bowden, "Heterojunction solar cells on flexible silicon wafers," *MRS Adv.*, vol. 1, no. 15, pp. 997–1002, 2016.